

# Holographic Entanglement Entropy in 2D Holographic Superconductor via $AdS_3/CFT_2$

Davood Momeni,<sup>1</sup> Hossein Gholizade,<sup>2</sup> Muhammad Raza,<sup>3,4</sup> and Ratbay Myrzakulov<sup>1</sup>

<sup>1</sup>*Eurasian International Center for Theoretical Physics and Department  
of General & Theoretical Physics, Eurasian National University,  
Astana 010008, Kazakhstan\**

<sup>2</sup>*Department of Physics, Tampere University of Technology  
P.O.Box 692, FI-33101 Tampere, Finland<sup>†</sup>*

<sup>3</sup>*Department of Mathematics, COMSATS Institute of Information Technology, Sahiwal 57000, Pakistan*

<sup>4</sup>*State Key Lab of Modern Optical Instrumentation,  
Centre for Optical and Electromagnetic Research,*

*Department of Optical Engineering, Zhejiang University, Hangzhou 310058, China<sup>‡</sup>*

(Dated: June 20, 2021)

The aim of the present letter is to find the holographic entanglement entropy (HEE) in 2D holographic superconductors (HSC). Indeed, it is possible to compute the exact form of this entropy due to an advantage of approximate solutions inside normal and superconducting phases with backreactions. By making the UV and IR limits applied to the integrals, an approximate expression for HEE is obtained. In case the software cannot calculate minimal surface integrals analytically, it offers the possibility to proceed with a numerical evaluation of the corresponding terms. We'll understand how the area formula incorporates the structure of the domain wall approximation. We see that HEE changes linearly with belt angle. It's due to the extensivity of this type of entropy and the emergent of an entropic force. We find that the wider belt angle corresponds to a larger holographic surface. Another remarkable observation is that no "confinement/deconfinement" phase transition point exists in our 2D dual field theory. Furthermore we observe that the slope of the HEE with respect to the temperature  $\frac{dS}{dT}$  decreases, thanks to the emergence extra degree of freedom(s) in low temperature system. A first order phase transition is detected near the critical point.

PACS numbers: 11.25.Tq, 03.65.Ud, 74.62.-c

*Introduction* Our contemporary physical questions are appearing a bit harder. Anti-de Sitter space/Conformal Field Theory (AdS/CFT) conjecture gives an abstract and still largely conjectural approach which applies in very general situations [1]. It stated: weakly coupled gravitational models at  $AdS$  bulk are dual to a strongly coupled CFT on boundary. This means that the strongly coupled quantum systems may correspond precisely to black holes. Gauge/gravity duality is a frequent application, particularly seen in those systems with strongly coupling, like type II superconductors [2]-[3]. The AdS/CFT movement seems particularly adept in its innovative approach to reality. Its areas of research interest include holographic superconductors, Quark-Gluon plasma, and superconductor/superfluid in condensed matter physics, particularly using qualitative approaches [4]-[7]. AdS/CFT has been used recently to produce a realistic model for entanglement quantum systems [8, 9] (with conformal field theory descriptions) with some success [10]-[24], as a geometric approach. In order to address this issues, we consider two possible portions  $\tilde{A}$ (set A),  $B = \tilde{A}'$  (the complementary set) of a single quantum system upon which an Hilbert space  $\mathcal{H}_{\tilde{A}} \times \mathcal{H}_{\tilde{A}'}$  may be based. We consider the Von-Neumann entropy

$S_X = -Tr_X(\rho \log \rho)$  the best of the best for statistical description, where  $Tr$  is the quantum trace of quantum operator  $\rho$  over quantum basis  $X$ . If we compute  $S_{\tilde{A}}$  and  $S_{\tilde{A}'}$ , this is extremely useful to see  $S_{\tilde{A}} = S_{\tilde{A}'}$ . A further consequence, however, is that Von-Neumann entropies are now more likely to identify it with a region, the boundary of  $\partial \tilde{A}$  [25]. More recently, studies on the role of analytical methods in computation of the EE have been initiated [26]-[28]. It must be specially an outstanding note in the role of this type of entropy to be specially computed to lower dimensional quantum systems as its  $AdS_3/CFT_2$  picture. Using a specially designed gravitational dual, we use EE to explain our 2D dynamical phase transitions. We'll investigate the reduced HEE of a strip geometry (belt) in three dimensional AdS background. It can be calculated analytically in terms of the cutoff length. The HEE and total length (angle) is approximated by a function for which the minimal surface integral is analytically solvable. After the normal form for the zero temperature has been derived, the extent to which the criticality regime  $T \sim T_c$  may be solved analytically is covered. In case the hand cannot calculate surface integrals analytically it offers the possibility to proceed with a numerical evaluation of the corresponding integrals. The variation in aggregation of the HEE illustrates a magnifying ability to adapt different phase transitions. At this point in the system the superconducting phase is preferred to the normal phase, thereby presenting the minimal surface area.

*Model for 2D HSC* The following action combines the

\*Electronic address: d.momeni@yahoo.com

<sup>†</sup>Electronic address: hosein.gholizade@gmail.com

<sup>‡</sup>Electronic address: mraza@zju.edu.cn

accuracy of AdS bulk modeling with the 2D quantum system on boundary [29]-[34]:

$$S = \int d^3x \sqrt{-g} \left[ \frac{1}{2\kappa^2} (R + \frac{2}{L^2}) - \frac{1}{4} F^{ab} F_{ab} - |\nabla\phi - iA\phi|^2 - m^2|\phi|^2 \right]. \quad (1)$$

Here,  $\kappa^2$  defines the three dimensional gravitational constant  $\kappa^2 = 8\pi G_3$ , the Newton constant  $G_3$ ,  $L$  is the AdS radius,  $m^2 = m_\phi^2 \in (-1, \infty)$  mass of scalar field, and  $g = \det(g_{\mu\nu})$ . For more accurate information we may also choose to fix a metric to AdS bulk over a given range of coordinates:

$$ds^2 = -f(r)e^{-\beta(r)} dt^2 + \frac{d\gamma^2}{f(r)} + \frac{r^2}{L^2} dx^2. \quad (2)$$

We may choose a temperature for CFT from our AdS black hole:

$$T = \frac{f'(r_+)e^{-\beta(r_+)/2}}{4\pi}. \quad (3)$$

We can adapt any conventional information by substituting static functions for gauge field  $A_\mu$  and scalar field  $\phi$  for bulk:

$$A_t = A(r)dt, \quad \phi \equiv \phi(r). \quad (4)$$

We can also use static symmetry to adapt our metric to best showcase the normal state of our system in the absence of scalar field:

$$f(r) = k + \frac{r^2}{L^2} - \kappa^2 \mu^2 \log r, \quad (5)$$

$$A(r) = \rho + \mu \log r. \quad (6)$$

where  $k = -\frac{r_+^2}{L^2} + \kappa^2 \mu^2 \log r_+$ ,  $\mu, \rho$  correspond to the chemical potential and charge density in the dual field theory respectively. Here,  $r_+$  is the radius  $r$  of the event horizon  $f(r_+) = 0$  for a AdS black hole. The fields  $A_\mu, \phi$  will satisfy regularity if they satisfy these auxiliary boundary conditions:

$$A(r_+) = 0, \quad \phi'(r_+) = \frac{m^2}{f'(r_+)} \phi(r_+), \quad (7)$$

and the metric ansatz satisfies:

$$f'(r_+) = \frac{2r_+}{L^2} - 2\kappa^2 r_+ \left[ m^2 \phi(r_+)^2 + \frac{1}{2} e^{\beta(r_+)} A'(r_+)^2 \right] \quad (8)$$

$$\beta'(r_+) = -4\kappa^2 r_+ \left[ \frac{A'(r_+)^2 \phi(r_+)^2 e^{\beta(r_+)}}{f'(r_+)^2} + \phi'(r_+)^2 \right] \quad (9)$$

The AdS asymptotic expansions for the fields, (5,6), require the values of:

$$\begin{aligned} \beta \rightarrow 0, \quad f(r) &\sim \frac{r^2}{L^2}, \quad A(r) \sim \mu \log r, \\ \phi(r) &\sim \frac{\langle \mathcal{O}_- \rangle}{r^{\Delta_-}} + \frac{\langle \mathcal{O}_+ \rangle}{r^{\Delta_+}}, \quad \text{as } r \rightarrow \infty. \end{aligned} \quad (10)$$

The use of  $\Delta_\pm$  can denote conformal dimensions  $\Delta_\pm = 1 \pm \sqrt{1 + m^2}$ . Let  $\langle \mathcal{O}_\pm \rangle$  denote the standard vacuum expectation values (VEV) of dual operators  $\mathcal{O}_\pm$  in CFT. A change of variable  $z = \frac{r_+}{r}$  has been applied, which essentially simplifies the forms of the equations of motion:

$$\phi'' + \frac{\phi'}{z} \left[ 1 + \frac{zf'}{f} - \frac{z\beta'}{2} \right] + \frac{r_+^2 \phi}{z^4} \left[ \frac{A^2 e^\beta}{f^2} - \frac{m^2}{f} \right] = 0, \quad (11)$$

$$A'' + \frac{A'}{z} \left[ 1 - \frac{z\beta'}{2} \right] - \frac{2r_+^2 A \phi^2}{z^4 f} = 0, \quad (12)$$

$$\beta' - \frac{4\kappa^2 r_+^2}{z^3} \left[ \frac{A^2 \phi^2 e^\beta}{f^2} - \frac{z^4 \phi'^2}{r_+^2} \right] = 0, \quad (13)$$

$$f' - \frac{2r_+^2}{L^2 z^3} - \kappa^2 z e^\beta A'^2 - \frac{2\kappa^2 m^2 r_+^2 \phi^2}{z^3} = 0, \quad (14)$$

$$-\frac{2\kappa^2 r_+^2}{z^3} \left[ \frac{A^2 \phi^2 e^\beta}{f} + \frac{f \phi'^2 z^4}{r_+^2} \right] = 0,$$

Solving the above equation with  $\phi \neq 0, T < T_c$  is the principal purpose of the superconductivity program [29, 30].

*HEE proposal* : Following to the proposal [8, 9], suppose a field theory in  $(d)D$  has a gravitational dual embedded in  $AdS_{d+1}$  bulk. The holographic algorithm is then used to compute the entanglement entropy of a region of space  $\tilde{A}$  and its complement from the  $AdS_{d+1}$  geometry of bulk:

$$S_{\tilde{A}} \equiv S_{HEE} = \frac{Area(\gamma_{\tilde{A}})}{4G_{d+1}}, \quad (15)$$

We first compute the minimal  $(d-1)D$  mini-super surface  $\gamma_{\tilde{A}}$ . It had been proposed to extend  $\gamma_{\tilde{A}}|_{AdS_{d+1}}$  to bulk, but with criteria to keep surfaces with same boundary  $\partial\gamma_{\tilde{A}}$  and  $\partial\tilde{A}$ . The equal boundary is the leading technique working to compute HEE via AdS/CFT.

Several options for the parametrization of the  $\tilde{A}$  are available as well as different choices for the  $\partial\gamma_{\tilde{A}}$  in the bulk. We discuss the possibility of computing HEE of 2D systems using parametric representation in one degree of freedom  $\tilde{A} := \{t = t_0, -\theta_0 \leq \theta \leq \theta_0, r = r(\theta)\}$ . Minimization can be used on Lagrangian which has a simple Beltrami form:

$$\mathcal{L} \equiv \sqrt{r^2 + \frac{r'(\theta)^2}{f(r)}} \quad (16)$$

Using the Beltrami identity, since  $\partial_\theta \mathcal{L} = 0$ , computations were taken by using a constant quantity  $\mathcal{L} - r' \partial_{r'} \mathcal{L} = C$  designed for  $\mathcal{L}^1$ .

In this case, we define half of the total length (angle)  $\theta_0$  and HEE in the more conventional forms, using the

<sup>1</sup> We can call it "Energy".

shorter list enumerated here:

$$\theta_0 = \int_0^{\theta_0} d\theta = \int_0^{\theta_0} \frac{Cdr}{r\sqrt{f(r)(r^2 - C^2)}} \quad (17)$$

$$S_{HEE} \equiv \frac{1}{2G_3} \int_0^{\theta_0} \frac{rdr}{\sqrt{f(r)(r^2 - C^2)}} \quad (18)$$

The aim of this letter is to evaluate the sensitivity of (17,18) in the bulk of acute regimes of temperature.

*Sharp domain wall approximation:* Studies are currently underway to develop and evaluate (17,18) using numerical algorithms. Our aim is to evaluate the (17,18) as an analytic tool. The (17,18) are determined from the domain wall approximation analysis [35]. Domain wall idea is proposed to investigate some aspects of the HEE along renormalization group (RG) trajectories. The RG flow is defined as the  $N = 1$  SUSY deformation of  $N = 4$  SUSY-YM theory. The geometry (metric) which we will use is called here domain wall geometry. These are Riemannian  $3D$  spaces which are assumed to be asymptotically AdS. The RG is a flow from one dual geometry in the UV to another in the IR. These regions are separated by an intermediate border, which can be realized as a domain wall, which is connecting the two regions. The position of such domain wall and its thickness are functions of the dual field theory parameters like dual charge density  $\rho$  or dual chemical potential  $\mu$ . What we want to understand is how the HEE incorporates the structure of the domain wall. Furthermore we want to know which kind of the field theory quantities are encoded in domain wall parameters. In our  $CFT_2$  case the RG flow is  $(1+1)D$  and we suppose that the bulk geometry  $AdS_3$  is idealized by a sharp domain wall medium. The domain wall is separating two  $AdS_3$  regions via two different values for the cosmological constant. What we want to obtain is the form of HEE (18) and belt angle (17) incorporate the structure of the domain wall. We consider the  $AdS_3$  is relating to RG flows in  $(1+1)D$ . For the AdS radius in two regions, we suppose that  $L_{IR} > L_{UV}$ . Furthermore we suppose that the length scale of AdS  $L$ , is defined as the following:

$$L = \begin{cases} L_{UV}, & r > r_{DW} \\ L_{IR}, & r < r_{DW} \end{cases} \quad (19)$$

Suppose we have a sharp phase transition between two patches of the AdS space time. We will try to locate it at  $r = r_{DW}$ . Here  $r_{DW}$  defines the position of the domain wall in the AdS radial direction. Indeed, in the massless limit,  $m^2 = 0$ , there exists an intermediate radius  $-\infty < r_m < 0$  such that  $\phi'(r_m) = 0$ . The ideal candidate for  $r_{DW}$  should be  $r_{DW} = r_m$ . We always assume that  $r_{DW} < 0$ . So we assume that the following form is a perfectly good tool for analytical evaluation:

$$C \equiv \frac{r^2}{\sqrt{r^2 + \frac{r'(\theta)^2}{f(r)}}} = \begin{cases} L_{UV}, & r > r_{DW} \\ L_{IR}, & r < r_{DW} \end{cases} \quad (20)$$

In the previous equation we took into account two different AdS radii,  $L_{UV}$  and  $L_{IR}$  in each region. With the previous considerations, the equations (17,18) are easily integrated,

$$\int_0^{\theta_0} d\theta = \theta_0 = \theta_{IR} + \theta_{UV}, \quad (21)$$

$$\theta_{IR} = \int_{r_*}^{r_{DW}} \frac{L_{IR}dr}{r\sqrt{f_{IR}\sqrt{r^2 - L_{IR}^2}}}, \quad (22)$$

$$\theta_{UV} = \int_{r_{DW}}^{r_{UV}} \frac{Ldr}{r\sqrt{f_{UV}\sqrt{r^2 - L^2}}} \quad (23)$$

here  $r_*$  denotes the ‘‘turning’’ point of the minimal surface  $\gamma_{\bar{A}}$ . It is defined by  $r'(\theta)|_{r=r_*} = 0$ . So we can choose to engage turning point with  $r_+$  or  $C$ . We replaced the integrating out to  $r = +\infty$  by integrating out to large positive radius  $r_{UV}$ . Indeed, we assume that  $r_{UV}$  stands out for UV cutoff [28]. We will suppose that  $r_* < r_{DW}$ . It means that the minimal surface drift onto the IR region. We can rewrite HEE as we like:

$$S_{HEE} = \frac{1}{2G_3} [S_{IR} + S_{UV}], \quad (24)$$

$$S_{IR} = \int_{r_*}^{r_{DW}} \frac{rdr}{\sqrt{f_{IR}(r^2 - L_{IR}^2)}}, \quad (25)$$

$$S_{UV} = \int_{r_{DW}}^{r_{UV}} \frac{rdr}{\sqrt{f_{UV}(r^2 - L_{UV}^2)}}. \quad (26)$$

In both cases IR,UV, the geometry of AdS has imposed tight constraints on the metric:

$$f(r) \rightarrow f_{IR} = 1, \text{ as } r \rightarrow -\infty. \quad (27)$$

$$f(r) \rightarrow f_{UV} = \frac{r^2}{L^2}, \text{ as } r \rightarrow \infty, \quad (28)$$

Perhaps we'll compute the  $\theta_{IR}, \theta_{UV}$  for another purpose:

$$\theta_{IR} = i \log \left[ \frac{r_* \sqrt{L_{IR}^2 - r_{DW}^2} - L_{IR}}{r_{DW} \sqrt{L_{IR}^2 - r_*^2} - L_{IR}} \right], \quad (29)$$

$$\theta_{UV} = \frac{\sqrt{r_{UV}^2 - L^2}}{r_{UV}} - \frac{\sqrt{r_{DW}^2 - L^2}}{r_{DW}}. \quad (30)$$

The entanglement entropy can be computed as the following:

$$S_{IR} = \sqrt{r_{DW}^2 - L_{IR}^2} - \sqrt{r_*^2 - L_{IR}^2} \quad (31)$$

$$S_{UV} = \frac{iL^2}{L_{UV}} \log \left[ \frac{r_{DW} \sqrt{L_{UV}^2 - r_{UV}^2} - L_{UV}}{r_{UV} \sqrt{L_{UV}^2 - r_{DW}^2} - L_{UV}} \right] \quad (32)$$

We consider two regimes, the IR and UV:

**UV limit:** we first consider  $r_* > r_{DW}$ . This showed that  $\gamma_{\bar{A}}$  were already embedding deeply into the  $AdS_3$  with boundary  $r \rightarrow \infty$ . To get a rough approximation of how much entropy in the  $\gamma_{\bar{A}}$  would be in UV limit, we simplify the problem by putting  $\theta_{IR} = S_{IR} = 0$  and identifying  $r_{DW} = r_*$  in Eqs. (23) and (25):

$$\theta_{UV} \sim -\frac{1}{2}\left(\frac{L}{r_{UV}}\right)^2, \text{ as } r_{UV} \rightarrow \infty \quad (33)$$

$$S_{UV} \sim (\pi \mp \frac{\pi}{2})\frac{L^2}{L_{UV}}, \text{ as } r_{UV} \rightarrow \infty \quad (34)$$

The second term is written to indicate the presence of black hole (BH) area entropy. The first term indicate clearly that the classical BH entropy is reduced through quantum effects.

**IR limit:** In case  $r_* \ll r_{DW}$ , i.e. the  $\gamma_{\bar{A}}$  extends deeply into the IR region. From Eqs. (22), (23), (25) and (26) we obtain:

$$\frac{\theta_0}{2} = -\frac{\pi}{2} - \frac{\sqrt{r_{UV}^2 - L^2} - r_{UV}}{r_{UV}}, \text{ as } r_* \rightarrow -\infty, \quad (35)$$

$$\lim_{r_* \rightarrow -\infty} S_{IR}^{\text{finite}} = r_{DW}, \quad (36)$$

$$S_{UV} = \frac{L^2}{r_{DW}} \quad (37)$$

$$+ \frac{iL^2}{L_{UV}^2} \log \left( \frac{iL_{UV} + \sqrt{r_{UV}^2 - L_{UV}^2}}{r_{UV}} \right)$$

Perhaps not surprisingly,  $S_{\text{finite}}^{HEE,IR} = \frac{r_{DW}}{2G_3}$  is exactly the result we would have computed if we were purely in the IR theory. It's interesting to note that IR limit can't follow the similar UV form. However according to the note above the BH area term calculated in IR limit is  $S_{HEE} = S_{BH} = \frac{r_{DW}}{2G_3} + \frac{L^2}{2G_3 r_{DW}}$ , so there is a difference for this regime. Note that there were major differences in the BH term in both regimes.

We mention here that because  $L_{IR} > L_{UV}$ , so we conclude that the dominated part of HEE is the one which is calculated in the IR limit given by  $S_{IR} \sim \frac{L^2}{r_{DW}} \sim L_{IR}$ , however  $S_{UV} \sim L_{UV} < S_{IR}$  which is obviously less than  $S_{IR}^2$ .

*HEE close to the  $T \lesssim T_c$  in the absence of scalar field  $\phi(z) = 0$ :* The normal phase can even be achieved from a list of functions:

$$\phi_0 = \beta_0 = 0, \quad A_0 = -\mu_c \log z, \quad (38)$$

$$f_0 = \frac{r_{+c}^2}{L^2} (z^{-2} - 1) + \kappa^2 \mu_c^2 \log z. \quad (39)$$

The EE between  $\tilde{A}$  and its complement is given by:

$$s_{\tilde{A}} = 4G_3 S_{HEE} = 2r_*^{-1} \int_{r_{UV}}^{r_*} \frac{r dr}{\sqrt{f(r)(r^2 - r_*^2)}} \quad (40)$$

The technique of this computation was a rewrite of  $s_{\tilde{A}}$  with better coordinate  $z$ :

$$s_{\tilde{A}} = 2r_+ r_* \int_{z_{UV}}^{z_*} \frac{dz}{z^3 \sqrt{f(z)} \sqrt{z^{-2} - z_*^{-2}}}. \quad (41)$$

The vicinity of the critical point  $T \lesssim T_c$  maybe served as a place for an equivalent form of integral:

$$s_{\tilde{A}} = 2r_{+c} r_* \int_{z_{UV}}^{z_*} \frac{dz}{z^3 \sqrt{f_0} \sqrt{z^{-2} - z_*^{-2}}}. \quad (42)$$

and

$$\frac{\theta_0}{2} = r_* \int_{r_{UV}}^{r_*} \frac{dr}{r \sqrt{f(r)(r^2 - r_*^2)}} \quad (43)$$

$$= \frac{r_*}{r_+} \int_{z_{UV}}^{z_*} \frac{dz}{z \sqrt{f(z)(z^{-2} - z_*^{-2})}}.$$

At criticality  $T \lesssim T_c$ :

$$\frac{\theta_0}{2} = \frac{r_*}{r_{+c}} \int_{z_{UV}}^{z_*} \frac{dz}{z \sqrt{f_0(z^{-2} - z_*^{-2})}}. \quad (44)$$

where

$$T_c = \frac{1}{4\pi r_{+c}} \left( 2r_{+c}^2 L^{-2} - \kappa^2 \mu_c^2 \right) \quad (45)$$

We go on to calculate the critical value of the horizon  $r_+$  used by  $\{T_c, \mu_c, \kappa^2\}$ :

$$\frac{r_{+c}}{L} = \pi T_c L + \frac{1}{2} \sqrt{4\pi^2 T_c^2 L^2 + 2\kappa^2 \mu_c^2}. \quad (46)$$

Parametric estimation of the (42,44) using polynomials is needed. We apply series method to estimation of  $\frac{1}{\sqrt{f(z)}}$  in (42,44). Expansion of the  $\frac{1}{\sqrt{f(z)}}$  as follows :

$$\frac{1}{\sqrt{f_0}} = \sum_{n=0}^{\infty} b_n \frac{(\log z)^n}{(z^{-2} - 1)^{n+1/2}}, \quad (47)$$

$$b_n = \frac{(\kappa \mu_c)^{2n} (-1)^n (1/2)_n \left( \frac{L}{r_{+c}} \right)^{2n+1}}{n!} \quad (48)$$

allows us to expand into the series the (42,44). We first evaluate a value of integral  $I_a^n$  for use in the (42,44) :

$$I_a^n \equiv \int_{z_{UV}}^{z_*} \frac{(\log z)^n dz}{z^a \sqrt{z^{-2} - z_*^{-2}} (z^{-2} - 1)^{n+1/2}}, \quad (49)$$

for  $a = 1, 3$

<sup>2</sup> The point is that these geometries are meant to represent an RG flow. For high energies (the UV of the theory), the background looks like planar AdS (and hence the  $N = 4$  SYM theory), whereas at low energies (the IR of the theory), the background looks like a different AdS (the low-energy limit of the field theory). The domain wall approximation was meant to be a toy model of the superconducting backgrounds [36].

The aim is to evaluate the integral of  $I_a^n$  as a series tool for interval  $0 \lesssim z_{UV} < z < z_* \lesssim 1$ :

$$I_a^n = \sum_{\alpha,\beta,\gamma=0}^{\infty} \frac{(1/2)_\alpha (n+1/2)_\beta}{\alpha! \beta! \gamma! (\gamma+n)} \quad (50)$$

$$\times \left( 2(\alpha + \beta + n) - a + 3 \right)^\gamma \left[ (\log z_*)^{\gamma+n} - (\log z_{UV})^{\gamma+n} \right]$$

here  $(a)_n \equiv \frac{(a+n-1)!}{n!(a-1)!}$  is the Pochhammer symbol [37].

We need to carefully evaluate (42,44) with  $I_a^n$ :

$$\frac{\theta_0}{2} = \frac{r_*}{r_{+c}} \sum_{n=0}^{\infty} b_n I_1^n, \quad (51)$$

$$s_{\bar{A}} = 2r_{+c} r_* \sum_{n=0}^{\infty} b_n I_3^n. \quad (52)$$

Indeed, the functions  $\theta' \equiv \frac{\theta_0}{2}$ ,  $s' \equiv \frac{s_{\bar{A}}}{r_{+c}^2}$  have the simple

forms in their bi-parametric  $\left( \frac{T}{T_c}, \frac{\mu}{\mu_c} \right)$  list:

$$s' = \frac{2\frac{T}{T_c} + \sqrt{4\left(\frac{T}{T_c}\right)^2 + \frac{2\zeta^2}{T_c^2 \pi^2 L^2} \left(\frac{\mu}{\mu_c}\right)^2}}{1 + \frac{1}{2} \sqrt{4 + \frac{2\zeta^2}{(\pi L T_c)^2}}} \sum_{n=0}^{\infty} B_n I_3^n \quad (53)$$

$$\theta' = \frac{\frac{T}{T_c} + \frac{1}{2} \sqrt{4\left(\frac{T}{T_c}\right)^2 + \frac{2\zeta^2}{T_c^2 \pi^2 L^2} \left(\frac{\mu}{\mu_c}\right)^2}}{1 + \frac{1}{2} \sqrt{4 + \frac{2\zeta^2}{(\pi L T_c)^2}}} \sum_{n=0}^{\infty} B_n I_1^n \quad (54)$$

as they may have the parameters  $\zeta = (\kappa \mu_c) = 0.005$ ,  $L \equiv 1$  and

$$B_n = \frac{\zeta^n (-1)^n (1/2)_n}{n!} \quad (55)$$

$$\times \left( \pi T_c L + \frac{1}{2} \sqrt{4 \pi^2 T_c^2 L^2 + 2\zeta^2} \right)^{-(2n+1)}.$$

For numerical calculations we set the  $T_c = 0.01$ . If in equations (53) and (54), we define the  $h_1(n) = \sum_{m=0}^n B_m I_3^m$  and  $h_2(n) = \sum_{m=0}^n B_m I_1^m$  then we can show the  $h_1$  and  $h_2$  as a function of  $n$  in figure (1). We choose

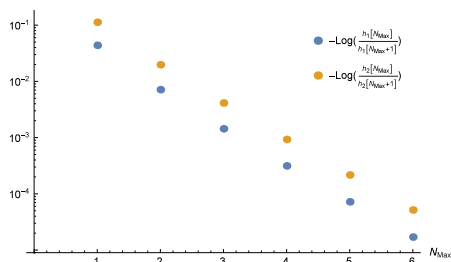


FIG. 1: The dependence of  $h_1$  and  $h_2$  functions on the upper limit of summation  $n = N_{Max}$  in equations (54) and (53). As one can see, the logarithm difference between  $n = 5$  and  $n = 6$  summations is less than  $10^{-4}$ . Therefore, we choose the  $n = 6$  as a series truncation in our calculations. This graph is for  $T_c = 0.01$ .

the  $n = 6$  as high value for  $n$ , because we can omit the relative error arising from series truncation.

An example (53) plot of reduced HEE in a system is shown in figure (2). Numeric analysis showed a significant smooth relationship between increasing proportions of  $\mu, T$  and increased  $s'$  in the this phase. Seeing an increasing HEE for system, it decided to become a normal conductor than just a superconductor. Increasing temperature to reduce HEE adds to the system a criticality, thus slowing the superconducting.

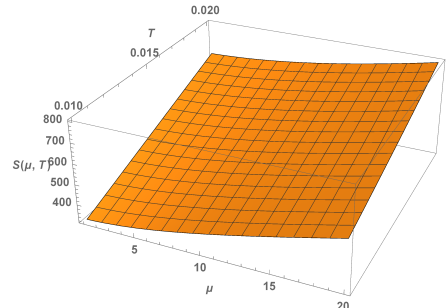


FIG. 2: Plot of the surface (53) versus  $\mu, T$ . It shows that  $s'$  is a monotonic-increasing function. It always increasing or remaining constant, and never decreasing.

It produces a regular phase of matter for  $T > T_c$ . Regular attendance at these non superconducting phase has proved numerically. Boundary conditions and regular tiny backreactions  $\zeta$  will help to keep normal phase for longer. Normal phase increasing the entropy (53), increases the hardenability of superconductivity.

We plot isothermal curves of (53) for various values of  $T$  in figure (3). Attending at least one lower temperature regime  $T < T_c$  is almost compulsory for superconductivity. We don't detect any local maxima for  $\frac{\mu}{\mu_c}$ . Consequently no "confinement/deconfinement" phase transition point exists in our 1 + 1 dual theory.

For fixed relative chemical potential  $\frac{\mu}{\mu_c}$ , we plot (53) as function of  $T$  in figure (4). We observe that at fixed  $\frac{\mu}{\mu_c}$ , one may increase the  $s'(T)$  simply by increasing the  $T$ . Furthermore, we see that the slope of the HEE with respect to the temperature  $\frac{dS}{dT}$  decreases as the relative chemical potential  $\frac{\mu}{\mu_c} \neq 1$  decreases. We understand this through the fact that, in low temperature and  $\frac{\mu}{\mu_c} \neq 1$ , more degree of freedoms (dof) will condense. An emergent of new extra dof at low temperature is happening.

Figure (5) shows typical behaviors of (53,54) versus temperature  $T$  for fixed  $T_c$ . Both are always increasing with respect to the temperature  $T$ , and never decreasing. This type of monotonic-increasing behavior with  $T$  depends on thermodynamically stability condition, in which the heat capacity at constant size must be positive. These are relatively low temperature, holographic superconductors which contain a prepared HEE which can linearly be described for system. It has been suggested that where there is low temperature phase may be able to keep superconductivity with increased reduced entropy (53) rises.

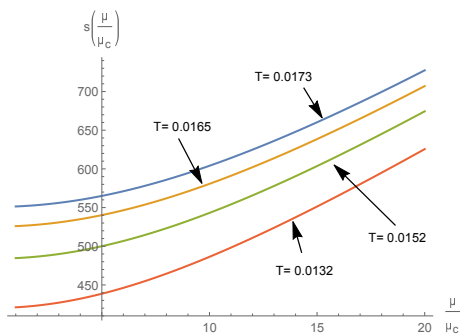


FIG. 3: Plot of the of the isothermal HEE (53) for various values of  $T$ . For positive values of the chemical potential,  $s'$  is a monotonic-increasing function, always increasing, and never decreasing. The "fixed" chemical potential will give a lower value of (53) for lower temperatures. At fixed temperature, in an isothermal graph, when  $\frac{\mu}{\mu_c}$  increases, the associated HEE entropy is also a monotonic-increasing function of  $\frac{\mu}{\mu_c}$ . Of course, attending at least one lower temperature regime  $T < T_c$  is almost compulsory for superconductivity. It was always realistic to expect that superconducting phase could be in being by lower values of  $\frac{\mu}{\mu_c}$  in isothermal regime. We don't detect any local maxima for  $\frac{\mu}{\mu_c}$ . Consequently no "confinement/deconfinemnet" phase transition point exists in our  $(1+1)D$  dual theory.

Figure (6) shows a linearly-dependent of reduced HEE (53) versus angle (54). The physical reason is that in small values of belt angle (small sizes) the system emerges new extra dof. A simple computational reason "why the  $s'$  can dominate on  $\theta'$ ", is that the main contribution (53,54) comes from the region  $r \sim r_* \sim r_+$  or  $z \sim z_*$ . A better more simple reason can be understood through the first law of thermodynamic for entanglement entropy. As we know, HEE behaves like a conventional entropy and it obeys the first law of thermodynamic [38],[39]. If we consider  $\theta'$  as the length scale of the system, then  $\frac{ds'}{d\theta'}$  is proportional to the entangled pressure  $P_E = T_E \frac{ds'}{d\theta'}$  at fixed temperature in the case of  $\frac{\mu}{\mu_c} > 1$ . A constant slope  $\frac{ds'}{d\theta'}$  gives us a uniform entangled pressure  $P_E$ . From the Maxwells relations we know that  $\left(\frac{ds'}{d\theta'}\right)_T = \left(\frac{dP}{dT}\right)_{\theta'}$ . It means that at fixed  $T$ , there is a uniform entropic gradient of HEE  $\left(\frac{ds'}{d\theta'}\right)$ . Consequently we obtain a uniform gradient of pressure  $\left(\frac{dP}{dT}\right)$  at fixed belt angle. A constant entropic force is emerged [38]. Another physical reason is that  $s'$  must be an extensive function of the "volume" or "size" of the entangled system, namely  $\theta'$ . Within the statistical mechanics there are extensive parameters like size, number of particles and thermodynamical functions like entropy. If we increase the size of the entangled system, here  $\theta' \rightarrow k\theta'$ , then the HEE  $s'$  must also increase. It means that  $s'$  must be a homogenous function of size.

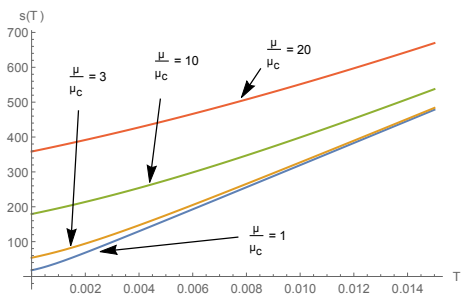


FIG. 4: Plot of (53) as function of  $T$  for various values of  $\frac{\mu}{\mu_c}$ . At fixed  $T$ , we may increase the  $s'(T)$  simply by increasing the  $\frac{\mu}{\mu_c}$ , or by increasing the number of Cooper (BCS) pair. Formation of the Cooper pairs decreases the extra dof of system. It is important to exclude  $\frac{\mu}{\mu_c} = 1$  for system. We should entirely exclude phase transition critical point  $\mu = \mu_c$  in our general study of HEE (53) against the cases  $\frac{\mu}{\mu_c} > 1$ . A somewhat amazing statement considering the HEE attempt to exclude the superconducting phase from the normal phase. This keyword can be used to exclude part of the criticality by entropy expression. At fixed  $\frac{\mu}{\mu_c}$ , one may increase the  $s'(T)$  simply by increasing the  $T > T_c$ . Furthermore we observe that the slope of the HEE with respect to the temperature  $\frac{ds'}{dT}$  decreases, thanks to the emergence extra dof in low temperature system.

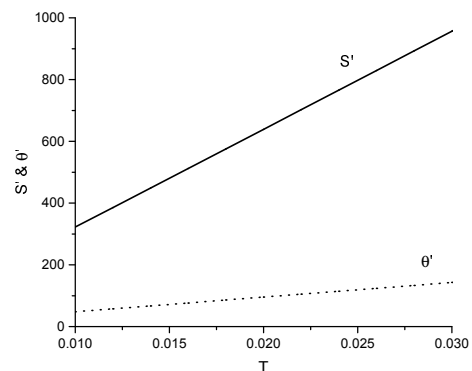


FIG. 5: The entanglement entropy (53) and the angle  $\theta'$  as a function of  $T$  for fixed  $\frac{\mu}{\mu_c}$ .

In this case,  $s'$  is found to be homogenous of first order, i.e.  $s'(k\theta') = ks'(\theta')$ . Consequently  $s' \sim \theta'$  changes linearly with  $\theta'$ .

Figure (7) shows that there are low-impact angle (54) designed specifically for low temperature and chemical potential. Furthermore,  $\theta'$  is a monotonic-decreasing function of  $\mu, T$ .

*HEE in the presence of scalar field  $\phi(z) \neq 0$  at  $T \lesssim T_c$ :* During the critical phase transition,  $\epsilon \equiv \langle \mathcal{O}_{\pm} \rangle$  is sufficiently tiny to expand functions by the following series forms:

$$\phi = \sum_{k=1}^{\infty} \epsilon^k \phi_k, \quad A = \sum_{k=0}^{\infty} \epsilon^{2k} A_{2k}, \quad (56)$$

$$f = \sum_{k=0}^{\infty} \epsilon^{2k} f_{2k}, \quad \beta = \sum_{k=1}^{\infty} \epsilon^{2k} \beta_{2k}. \quad (57)$$

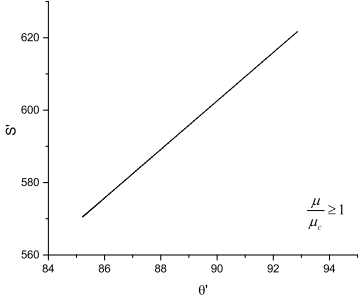


FIG. 6: The entanglement entropy (53) as a function of belt angle at fixed temperature in the case of  $\frac{\mu}{\mu_c} \geq 1$ .

We observe that HEE (53) is dominated by the connected minimal surface. The wider angle (54) corresponds to a larger surface holographic surface. We see that HEE (53) changes linearly with  $\theta'$ . A simple computational reason "why the  $s'$  can dominate on  $\theta''$ ", is that the main contribution (53,54) comes from the region  $r \sim r_* \sim r_+$  or  $z \sim z_*$ . Furthermore, there is no critical belt angle  $\theta'_c$  in which we can label the "confinement/deconfinement" transition point to it. The main reason is that the HEE is an extensive function of belt angle,  $s'(k\theta') = ks'(\theta')$ .

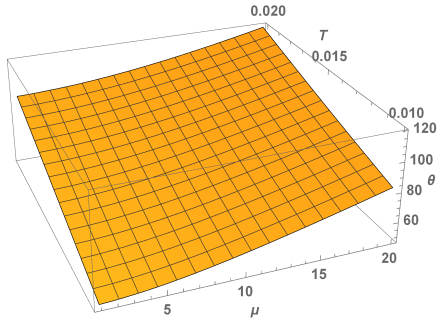


FIG. 7: 3D plot of  $\theta'$  as a function of  $\mu$  and  $T$ . It shows that  $\theta'$  is a monotonic-decreasing function.

When we turn-on the condensate,  $\phi(z) \neq 0$ , as we expect, analytical expression for HEE is much more harder. Specially at the criticality,  $T \lesssim T_c$ , because scalar field  $\phi(z)$  and Maxwell field  $A(z)$  backreacted on the metric functions  $f(z), \beta(z)$ . Generally speaking, one cannot solve field equations given in (11-15) and find the analytic form of  $f(z)$  in a closed form. However, the approximate solutions for (11-15) will be possible. We start by the following solutions:

$$\phi(z) = \epsilon\phi_1, A(z) = A_0 + \epsilon^2 A_2, \quad (58)$$

$$\beta(z) = \epsilon^2 \beta_2, f(z) = f_0 + \epsilon^2 f_2. \quad (59)$$

where  $\epsilon \equiv \langle \mathcal{O}_\pm \rangle$ . Analytical solutions obtained by

substituting (58,59) into the field equations (11-15):

$$f_2 = \left[ -2\kappa^2 \mu_c B + \kappa^2 B^2 + \frac{4r+c}{L^2} \right] (1-z) \quad (60)$$

$$+ \mathcal{O}((1-z)^2), \text{ as } T \lesssim T_c.$$

Which can be used according to the approximate solutions of the fields:

$$\phi_1 = \mu(1-z), \quad A_2 = B(1-z), \quad \beta_2''(1) = 0. \quad (61)$$

we can approximate the HEE and belt angle by putting a metric function through a carefully defined integrals:

$$s_{\bar{A}} = 2r_+ c r_* \int_{z_{UV}}^{z_*} \frac{dz}{z^3 \sqrt{f_0 + \epsilon^2 f_2} \sqrt{z^{-2} - z_*^{-2}}} \quad (62)$$

$$\frac{\theta_0}{2} = \frac{r_*}{r_+ c} \int_{z_{UV}}^{z_*} \frac{dz}{z \sqrt{(f_0 + \epsilon^2 f_2)(z^{-2} - z_*^{-2})}}. \quad (63)$$

where  $\epsilon \sim \sqrt{\mu - \mu_c} \sim \sqrt{1 - \frac{T}{T_c}} \ll 1$ .

Expansion of the  $\frac{1}{\sqrt{f_0 + \epsilon^2 f_2}}$  as follows :

$$\frac{1}{\sqrt{f_0 + \epsilon^2 f_2}} = \frac{1}{\sqrt{f_0}} \left( 1 - \frac{1}{2} \epsilon^2 \frac{f_2}{f_0} \right). \quad (64)$$

we obtain:

$$\frac{\theta_0}{2} = \frac{r_*}{r_+ c} \sum_{n=0}^{\infty} b_n \left( I_1^n - \frac{1}{2} \epsilon^2 \tilde{I}_1^n \right), \quad (65)$$

$$s_{\bar{A}} = 2r_+ c r_* \sum_{n=0}^{\infty} b_n \left( I_3^n - \frac{1}{2} \epsilon^2 \tilde{I}_3^n \right). \quad (66)$$

Where

$$\tilde{I}_a^n \equiv \int_{z_{UV}}^{z_*} \frac{f_2}{f_0} \frac{(\log z)^n dz}{z^a \sqrt{z^{-2} - z_*^{-2}} (z^{-2} - 1)^{n+1/2}}, \quad (67)$$

for  $a = 1, 3$

We rewrite them in terms of  $\left( \frac{T}{T_c}, \frac{\mu}{\mu_c} \right)$  as the following:

$$s' = \frac{\frac{2T}{T_c} + \sqrt{4\left(\frac{T}{T_c}\right)^2 + \frac{2\zeta^2}{T_c^2 \pi^2 L^2} \left(\frac{\mu}{\mu_c}\right)^2}}{1 + \frac{1}{2} \sqrt{4 + \frac{2\zeta^2}{(\pi L T_c)^2}}} \quad (68)$$

$$\times \sum_{n=0}^{\infty} B_n \left( I_3^n - \epsilon_0^2 \frac{1 - \frac{T}{T_c}}{2} \tilde{I}_3^n \right)$$

$$\theta' = \frac{\frac{T}{T_c} + \frac{1}{2} \sqrt{4\left(\frac{T}{T_c}\right)^2 + \frac{2\zeta^2}{T_c^2 \pi^2 L^2} \left(\frac{\mu}{\mu_c}\right)^2}}{1 + \frac{1}{2} \sqrt{4 + \frac{2\zeta^2}{(\pi L T_c)^2}}} \quad (69)$$

$$\times \sum_{n=0}^{\infty} B_n \left( I_1^n - \epsilon_0^2 \frac{1 - \frac{T}{T_c}}{2} \tilde{I}_1^n \right)$$

Here  $\epsilon_0 \ll 1$  is a numeric. The second negative term, seems obviously compatible with a superconductor phase

in the presence of the scalar field. By decreasing the amount of entropy produced in the superconductor phase, system alters the phase of conductivity.

For numerical calculations in (68) and (69) we must estimate the numerical errors. As figure (1), for low temperature region, in this case we have:

$$h_{1(2)}(N_{max}) = \sum_{n=0}^{N_{Max}} b_n (I_{3(1)}^n - \frac{\epsilon_0^2}{2} (1 - \frac{T}{T_c}) \tilde{I}_{3(1)}^n). \quad (70)$$

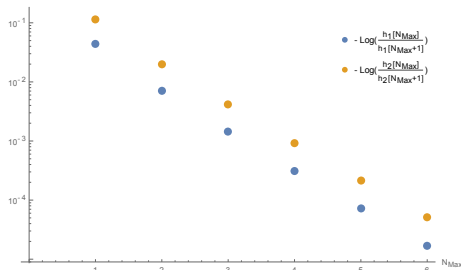


FIG. 8: The graph represent zero temperature case with  $T_c = 0.01$ , because it has the maximum difference with figure (1). Similar to figure (1), we choose  $N_{Max} = 6$ .

We plot (68) vs. (69). We adjust data as  $\epsilon_0^2 = 0.05$ ,  $\kappa\mu_c = 0.005$ . The critical temperature was obtained as  $T_c = 0.2$ . The system evolves from normal phase  $T > T_c$  to the superconductor phase  $T \lesssim T_c$  for  $T \approx 0.0179, 0.0173, 0.0165, 0.0152, 0.0132$ . The wider angle (69) corresponds to a larger surface holographic surface. We see that HEE (68) changes linearly with  $\theta'$ . We observe that the slope of the HEE with respect to the belt angle  $\frac{ds'}{d\theta'}$  remains constant. Like the non superconductor phase, here is no critical belt angle  $\theta'_c$  in which we can label the "confinement/deconfinement" transition point to it. The main reason is that the HEE is an extensive, homogenous (first order) function of belt angle,  $s'(k\theta') = ks'(\theta')$ .

*Phase transition at critical point*: A numerical study of (53),(68) shows that these solutions were smooth, and that their behaviors went most smoothly when the phase transition held the same mechanism as the usual. But after the system proceeded more smoothly, and the temperature of the system  $T$  regained his critical value  $T_c$  in the system, if the temperature alters as the  $T \simeq T_c$ , a discontinuity occurs in the  $\frac{ds'}{dT}$  when the phase is changed, and a first order phase transition may be introduced into the system. The difference between  $\frac{ds'}{dT}$  for  $T > T_c$  (eq.(53)) and  $T < T_c$  (eq.(68)) at  $T = T_c$  is plotted in figure (10) for a log-scaled entropy. The graph is obtained by smoothly connecting two graphs of  $s'(T)$  in the normal phase  $T > T_c$  i.e. the figure (5) and the one in the superconductor phase based on the formula given in (68). When we scaled the entropy in log scale, we observe a first order discontinuity in  $\frac{ds'}{dT}$  at the critical point  $T = T_c$ . Indeed, at the critical point  $\lim_{T \rightarrow T_c} \frac{ds'}{dT} = \infty$

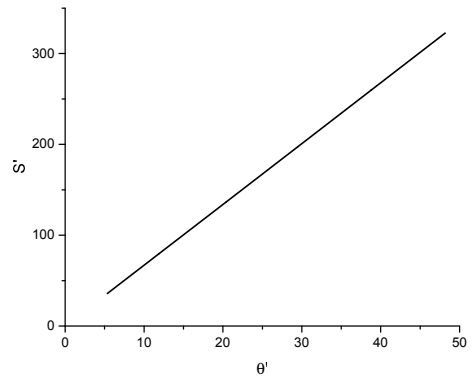


FIG. 9: Plot of  $s'$  (68) as a function of  $\theta'$  (69) for  $T \lesssim T_c$ . We adjust data as  $\epsilon_0^2 = 0.05$ . The critical temperature was obtained as  $T_c = 0.2$ . The system evolves from normal phase  $T > T_c$  to the superconductor phase  $T \lesssim T_c$ . The wider angle (69) corresponds to a larger holographic surface. We see that HEE (68) changes linearly with  $\theta'$ .

and  $\frac{ds'}{dT}|_{T>T_c} - \frac{ds'}{dT}|_{T<T_c} \simeq \sum_{n=0}^{\infty} B(n) \tilde{I}_3^n$ . We observe the first order phase transitions from the behavior of the entanglement entropy  $s'(T)$  at the critical point  $T = T_c$ . These types of first order phase transitions have been observed recently in literature [22]. We conclude that the HEE is indeed a good probe to phase transition in lower dimensional holographic superconductors. Furthermore, it implies that the HEE can indicate not only the occurrence of the phase transition, but also we can learn about the order of the phase transition from it.

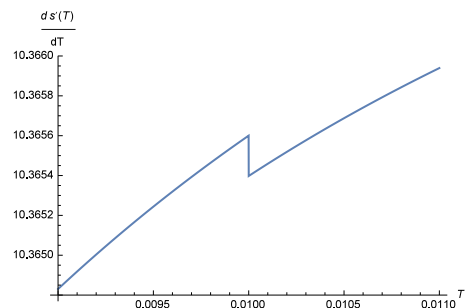


FIG. 10: Discontinuity in  $\frac{ds'}{dT}$  near critical point  $T_c = 0.01$ . We scaled the entropy in log-scale form.

*Summary*: The aim of this letter was to investigate the effect of superconductor critical phase transition in 2D models of holographic superconductors on holographic entanglement entropy. We investigate analytical aspects of the domain wall approximation and scalar condensate of the transition phases. Using the domain wall auxiliary asymptotic boundary conditions, as have been used before we can investigate the evolution of the holographic entanglement entropy for this superconductor model. To calculate the HEE in the critical phase first the interval is divided by the cutoffs in the UV and IR domains. Then



we have to resort the calculations of the holographic entanglement entropy in the presence of scalar field. It can be computed analytically in terms of the series functions of  $\mu, T$ . After the normal phase  $T > T_c$ , the superconductor phase  $T \lesssim T_c$  for the equations has been derived, the extent to which the equations may be solved analytically is covered. In case we cannot calculate minimal surface integrals analytically it offers the possibility to proceed with a numerical evaluation of the corresponding terms. We proceeded to investigate why the HEE increase with temperature and belt angle in the backreacted and normal  $AdS_3$  background. Both are always increasing with respect to the temperature  $T$  and belt angle  $\theta'$ , and never decreasing. This type of monotonic-increasing behavior with  $T$  depends on thermodynamical stability condition, in which the heat capacity at constant size must be pos-

itive. In the case of  $\theta'$ , there is no critical belt angle  $\theta'_c$  in which we can label the "confinement/deconfinement" transition point to it. The main reason is that the HEE is an extensive, homogenous (first order) function of belt angle,  $s'(k\theta') = ks'(\theta')$ . We observe the first order phase transitions from the behavior of the entanglement entropy  $s'(T)$  at the critical point  $T = T_c$ . We conclude that the wider belt angle corresponds to a larger surface holographic surface. Hopefully, the results of this study would come out until we could explore the roles of backreactions and scalar condensation on holographic entanglement entropy.

*Acknowledgments* We are indebted to the referee for pointing out the important comments and making suggestions for improvement of this work.

- 
- [1] J. Maldacena, Adv. Theor. Math. Phys. **2**, 231(1999)[Int. J. Theor. Phys. **38**, 1113 (1999)]
- [2] S. S. Gubser, Phys. Rev. D **78**, 065034(2008).
- [3] S. A. Hartnoll, C. P. Herzog, and G. T. Horowitz, Phys. Rev. Lett. **101**, 031601(2008)
- [4] C. P. Herzog, J. Phys. A **42**, 343001(2009)
- [5] G. T. Horowitz, Lect. Notes Phys. **828**, 313 (2011) [arXiv:1002.1722 [hep-th]].
- [6] R. G. Cai, L. Li, L. F. Li and R. Q. Yang, arXiv:1502.00437 [hep-th].
- [7] D. Momeni, M. Raza and R. Myrzakulov, arXiv:1410.8379 [hep-th].
- [8] S. Ryu and T. Takayanagi, Phys. Rev. Lett. **96**, 181602 (2006).
- [9] S. Ryu and T. Takayanagi, J. High Energy Phys. **0608**, 045 (2006).
- [10] T. Nishioka and T. Takayanagi, J. High Energy Phys. **0701**, 090 (2007).
- [11] I.R. Klebanov, D. Kutasov, and A. Murugan, Nucl. Phys. B **796**, 274 (2008).
- [12] A. Pakman and A. Parnachev, J. High Energy Phys. **0807**, 097 (2008). 13
- [13] T. Nishioka, S. Ryu, and T. Takayanagi, J. Phys. A **42**, 504008 (2009).
- [14] L.-Y. Hung, R.C. Myers, and M. Smolkin, J. High Energy Phys. **1104**, 025 (2011).
- [15] J. de Boer, M. Kulaxizi, and A. Parnachev, J. High Energy Phys. **1107**, 109 (2011).
- [16] N. Ogawa and T. Takayanagi, J. High Energy Phys. **1110**, 147 (2011).
- [17] T. Albash and C.V. Johnson, J. High Energy Phys. **1202**, 095 (2012).
- [18] R.C. Myers and A. Singh, J. High Energy Phys. **1204**, 122 (2012).
- [19] T. Albash and C.V. Johnson, J. High Energy Phys. **1205**, 079 (2012); arXiv:1202.2605 [hep-th].
- [20] X.M. Kuang, E. Papantonopoulos, and B. Wang, arXiv:1401.5720 [hep-th].
- [21] R.G. Cai, S. He, L. Li, and Y.L. Zhang, J. High Energy Phys. **1207**, 088 (2012); arXiv:1203.6620 [hep-th].
- [22] L. F. Li, R. G. Cai, L. Li and C. Shen, arXiv:1310.6239 [hep-th].
- [23] R.G. Cai, S. He, L. Li, and L.F. Li, J. High Energy Phys. **1210**, 107 (2012); arXiv:1209.1019 [hep-th].
- [24] W.P. Yao and J.L. Jing, arXiv:1401.6505 [hep-th].
- [25] M. Srednicki, Phys. Rev. Lett. **71**, 666 (1993) [hep-th/9303048].
- [26] Y. Peng and Q. Pan, JHEP **1406**, 011 (2014) [arXiv:1404.1659 [hep-th]].
- [27] Y. Ling, P. Liu, C. Niu, J. P. Wu and Z. Y. Xian, arXiv:1502.03661 [hep-th].
- [28] A. M. Garca-Garca and A. Romero-Bermdez, arXiv:1502.03616 [hep-th].
- [29] Y. Liu, Q. Pan and B. Wang, Phys. Lett. B **702**, 94 (2011) [arXiv:1106.4353 [hep-th]].
- [30] D. Momeni, M. Raza, M. R. Setare and R. Myrzakulov, Int. J. Theor. Phys. **52** (2013) 2773 [arXiv:1305.5163 [physics.gen-ph]].
- [31] Y. Bu, Phys. Rev. D **86** (2012) 106005 [arXiv:1205.1614 [hep-th]].
- [32] R. Li, Mod. Phys. Lett. A **27** (2012) 1250001.
- [33] T. Andrade, J. I. Jottar and R. G. Leigh, JHEP **1205** (2012) 071 [arXiv:1111.5054 [hep-th]].
- [34] A. J. Nurmagambetov, arXiv:1107.2909 [hep-th].
- [35] T. Albash and C. V. Johnson, JHEP **02** (2012) 95.
- [36] We are indebted to Tameem Albash for pointing out this comment.
- [37] M. Abramowitz, and I. A. Stegun, (Eds.). *Handbook of Mathematical Functions with Formulas, Graphs, and Mathematical Tables*, 9th printing. New York: Dover, 1972.
- [38] J. Bhattacharya, M. Nozaki, T. Takayanagi and T. Ugajin, Phys. Rev. Lett. **110**, no. 9, 091602 (2013) [arXiv:1212.1164].
- [39] D. Momeni, M. Raza, H. Gholizade and R. Myrzakulov, arXiv:1505.00215 [hep-th].